Rigid rotator under slowly varying kicks: Dynamic autoresonance and time-varying chaos

Baruch Meerson and Shalom Yariv

Center for Plasma Physics, Racah Institute of Physics, Hebrew University of Jerusalem, Jerusalem 91904, Israel
(Received 22 February 1991)

We investigate numerically and analytically the dynamics of a rigid rotator under the action of "kicks" with slowly varying strength and period. We derive a discrete map for this model and use the map to study three effects. The first of them is the dynamic autoresonance, which can lead to a significant regular acceleration or deceleration of the rotator. We find conditions for which the effect occurs, including the condition for an unlimited acceleration. The second effect is the transition to global chaos that arises due to the increase of the stochasticity parameter with time. We find that this transition occurs through bifurcation of the main island (the bifurcation parameter being simply time) and the development of a complicated separatrix structure. Also, slowly evolving global chaos is studied numerically, and a time-dependent analog of the "quasilinear" diffusion equation is shown to describe quite accurately the numerical simulations.

I. INTRODUCTION

The kicked-rotator model (and the "standard," or Chirikov-Taylor, mapping derived from it) describes a rigid rotator, kicked periodically by δ-function impulses. Being a very special model, it nevertheless proved to be rather useful in various physical problems. Also, it presents a good local approximation to a still larger number of systems (this justifies the name "standard mapping") and therefore has been extensively studied [1–3]. The standard mapping has the following form:

$$I_{n+1} = I_n + K \sin\theta_n , \tag{1}$$

$$\theta_{n+1} = \theta_n + I_{n+1} , \tag{2}$$

where I is the normalized action variable, θ is the phase variable, K is the parameter of the mapping (stochasticity parameter), and n is the discrete time. Mapping (1), (2) serves as one of the "working models" describing the transition from local to global chaos in time-dependent deterministic Hamiltonian systems with one degree of freedom. It was found that for K larger than approximately 0.97, the motion described by mapping (1), (2) becomes globally chaotic, while for $K < 0.97$ the chaos remains local [1–3].

The standard mapping (1), (2) refers to the simplest case when both the kick strength and the time interval between any two successive kicks (the kick period) are constant. In the present work we shall somewhat generalize this model and allow kicks with slowly varying strength and period. This complication of the model proves to be justified because it enables us to study three generic effects, which are absent in the standard map. The first of them can be called the dynamic autoresonance (DAR), and it refers to the regions of the phase space where the motion is regular. It presents a large (though completely regular) increase or decrease of the action variable I (the rotator acceleration or deceleration), caused by a slow monotonic variation in the kick

period. Different versions of this effect were studied in a number of applications and, first of all, in many charged particle acceleration schemes. Probably, the first theoretical work describing this effect was the classical work of Bohm and Foldy [4] on the theory of synchrotron. However, to the best of our knowledge, no attempts have been made before to consider the DAR in the framework of a simple mapping and thus considerably simplify the problem, otherwise too complicated for a detailed analytical analysis.

The second effect we are going to discuss is a direct descendent of the first. It can occur in nonlinear systems (oscillators or rotators) with a negative nonlinearity and presents "dragging" the system from local to global chaos via the DAR mechanism. Also, we shall consider the case of a well-developed global chaos to study the *nonstationary* diffusion of the action variable resulting from the slowly variation of the kicks. Such a nonstationary diffusion regime is characteristic of deterministically chaotic systems, parameters of which slowly vary in time, and this generally complicated problem looks much simpler in the framework of the mapping.

The organization of the paper is the following. In Sec. II we derive a "generalized standard mapping" for the problem of a kicked rotator with the variable kick strength and period. Then we apply the mapping to the case of a slowly decreasing kick period to demonstrate the DAR effect. In the same section we employ the isolated-resonance approximation, which helps one to better understand the effect. Section III is devoted to the case of a negative nonlinearity of the "rotator" and slowly increasing kick period. Here our numerical computations show a time-dependent transition to global chaos through a sequence of doubling and multiplying bifurcations, where the bifurcation parameter is simply time. The nonstationary diffusion occurring in the case of a well-developed global chaos is considered in Sec. IV. In Sec. V we present a simple example of a physical system which can be approximately described by the generalized

standard mapping. Finally, Sec. VI presents a brief summary of the results.

II. GENERALIZED STANDARD MAPPING AND THE DYNAMIC AUTORESONANCE

Let us consider the Hamiltonian function $H(I,\theta,t)$ of a nonlinear oscillator (or rotator) perturbed by θ-dependent δ-function impulses at some arbitrary time intervals $t_1,t_2,t_3,\ldots,t_k,\ldots$ ($t_i < t_j$ for $i < j$):

$$H(I,\theta,t)=H_0(I)+\cos\theta \sum_{k=-\infty}^{\infty} V_k \delta(t-t_k) \tag{3}$$

where V_k is the time-dependent strength of the kicks. I and θ are the action and angle variables, respectively, defined by the unperturbed oscillator with Hamiltonian $H_0(I)$. We can directly integrate the equations of motion following from the Hamiltonian (3) to find a mapping which expresses I and θ immediately before the $(n+1)$th kick in terms of these quantities immediately before the nth kick:

$$I_{n+1}=I_n+V_n\sin\theta_n , \tag{4}$$

$$\theta_{n+1}=\theta_n+\omega(I_{n+1})T_{n+1}(\mathrm{mod}2\pi) , \tag{5}$$

where $\omega=\partial H_0/\partial I$ is the unperturbed oscillation (rotation) frequency, $T_{n+1}=t_{n+1}-t_n$ is the time interval between two successive kicks $(n+1)$th and nth (the kick period). From now on phase θ will always be meant to be taken modulo 2π. It is seen that, in contrast to the standard mapping, parameters of mapping (4), (5) (i.e., V_n and T_{n+1}) depend explicitly on the discrete time n.

Let us start with the case of a positive nonlinearity. Further simplifying the problem, we assume the simplest dependence $\omega(I)=\omega_0+\omega'I$ with positive ω_0 and ω', and change variables from I to $I'=I+(\omega_0/\omega')$. In doing this we replace a general nonlinear oscillator by a rigid rotator. We will call variable I' "the physical action" and omit the prime in the following. Then, defining $\xi_n=\omega'T_n$, $K_{n+1}=V_n\xi_{n+1}$, and $\delta_{n+1}=(\xi_{n+1}-\xi_n)/\xi_n$, and transforming to a new variable $J_n=\xi_n I_n$, we arrive at the following mapping:

$$J_{n+1}=J_n+K_{n+1}\sin\theta_n+\delta_n J_n , \tag{6}$$

$$\theta_{n+1}=\theta_n+J_{n+1} \ (\mathrm{mod}2\pi) . \tag{7}$$

Mapping (6), (7) generalizes both the standard mapping (1), (2) and two more mappings, originating from the standard mapping. First, it is reduced to the standard mapping (1),(2) in the case of $T_n=$const and $V_n=$const. Indeed, in this case J_n becomes I_n multiplied by a constant, while $\delta_n=0$ and $K_{n+1}=$const.

Second, if T_n is kept constant, but V_n is not, mapping (6), (7) coincides with that considered by Dana and Reinhardt [5]. In this case $J_n=$const I_n and $\delta_n=0$, but $K_{n+1}\neq$const.

Finally, there is one particular case in which mapping (6), (7) takes the form of the "standard dissipative mapping," or Zaslavsky mapping [6]. This is the case when variations of V_n and ξ_n preserve the constancy of

$K_{n+1}=V_n\xi_{n+1}$, while δ_n is also constant. It means that both the kick period and the kick strength are varying with n according to some geometric progressions with reciprocal factors. The case of a normal (positive) dissipation corresponds to $\delta_n<0$. It should be mentioned that while mapping (4), (5) for the physical action I and phase θ is area preserving (therefore there is no real dissipation in the system), the term with δ_n causes dissipation in mapping (6), (7) for variables J and θ. Note also that the physical time t can be expressed in terms of the discrete time intervals in the following way:

$$t(n)=\sum_{k=1}^{n} T_k=\frac{1}{\omega'}\sum_{k=1}^{n}\xi_k . \tag{8}$$

In the following we are interested only in the case when variations in V_n and ξ_n are very slow, so that after a small number of iterations the mapping remains very close to the standard mapping (sometimes we shall have to impose more rigid conditions). This means, in particular, that δ_n is very small: $\delta_n \ll 1$. However, even in this case the term containing δ_n in Eq. (6) makes the mapping nonperiodic in J, in contrast to the standard mapping [mapping (4), (5) for the physical variables is nonperiodic in I also]. One of the important consequences of this fact is the absence in mappings (4), (5) and (6), (7) of the "accelerator modes" [1], which present a nongeneric curiosity of the standard mapping.

Our first aim is to demonstrate the DAR effect in mapping (6), (7). Let us start with an auxiliary mapping, which is obtained from mapping (6), (7) by setting $K_{n+1}=$const and $|\delta_n|=$const $\ll 1$. The auxiliary mapping has the following period-1 fixed points (θ_*,J_*): $J_*=2\pi l$, $\sin\theta_*=-2\pi l\delta_n/K_{n+1}$, where $l=0,1,2,\ldots$. For $\delta_n\neq0$ the number of the period-1 fixed points is always finite and equal to $l_{\max}+1$, where $l_{\max}$ is the maximum value of l for which

$$2\pi l|\delta_n|/K_{n+1}<1 . \tag{9}$$

We shall call the islands, corresponding to the stable period-1 fixed points of the auxiliary mapping, "the main islands." Only those fixed points are stable (they are stable foci) for which

$$\theta_*=\pi+\arcsin(2\pi l\delta_n/K_{n+1}) . \tag{10}$$

The tangent mapping, obtained from the auxiliary mapping in the vicinity of any of the stable period-1 fixed points, has two complex conjugate eigenvalues with the following absolute values:

$$|\lambda_{1,2}|=(1+\delta)^{1/2} . \tag{11}$$

Assume that for all n, K_{n+1} is less than the critical value $K_{\mathrm{crit}}(l)$ at which the lth period-1 fixed point loses its linear stability:

$$K_{n+1}<K_{\mathrm{crit}}(l)=(4+2\delta)/\cos\theta_* . \tag{12}$$

It is natural to assume that for $\delta_n\ll K_n$ and small enough values of l, the size of the area from which trajectories of the auxiliary mapping are attracted to the corresponding stable focus is close to the size of the main is-

lands of the standard mapping. In other words, the majority of points lying within the lth main island are mapped by the auxiliary mapping to points lying within the same island. Now, let us apply mapping (6), (7) with variable K_{n+1} and δ_n to a point lying within an island not too close to the island border. If we change parameters K_{n+1} and δ_n with n sufficiently slowly (the characteristic time of these changes must be larger than the "nonlinear" period of the particle motion inside the island; see Sec. III), and if K_{n+1} remains lower than $K_{\mathrm{crit}}(l)$, we can expect the motion to continue being regular and confined within the (adiabatically evolving) island. In particular, period-1 fixed points of the auxiliary mapping will become adiabatically evolving period-1 "quasifixed" points. In other words, the average value of J_n, which we will denote by $\langle J_n \rangle$, will remain constant and equal to J_*. Then, going back to the physical action $I_n = J_n / \xi_n$, we immediately obtain the following simple, but important result:

$$\langle I_n \rangle = 2\pi l \xi_n^{-1} . \tag{13}$$

Since ξ_n is proportional to T_n, we see that by slowly decreasing (increasing) the kick period, we can significantly increase (decrease) $\langle I_n \rangle$, that is, accelerate (decelerate) the rotator. The necessity to *decrease* T_n in order to *accelerate* results from the positiveness of the rotator nonlinearity.

Equation (13) can be rewritten as a DAR condition:

$$l\Omega_n = \omega(\langle I_n \rangle) , \tag{14}$$

where $\Omega_n = 2\pi / T_n$ is the time-dependent angular kick frequency. Therefore, despite large (but sufficiently slow) variations of the driving frequency Ω_n, the rotator frequency remains locked in the lth resonance, which can be called DAR acceleration/deceleration. It is important that relations (13), (14) are independent of the initial conditions, i.e., the same resonance involves a large fraction of trajectories, initially lying within the island. DAR is also possible for higher harmonics of frequency ω. For example, the second-harmonic resonance condition has the following form:

$$l\Omega_n = 2\omega(\langle I_n \rangle) , \tag{15}$$

which corresponds to the (slowly evolving) period-2 quasifixed points of mapping (6), (7).

All these considerations are supported by numerical simulations, as can be seen from Figs. 1–3. Here are shown three typical examples [denoted by (a), (b), and (c)], of the DAR acceleration on the third, second, and first harmonic, respectively, as described by the generalized standard mapping (6), (7). All the three examples have the common set of parameters $\delta_n = -0.005 = \mathrm{const}$ and $K_n = 0.995^n$ (that is, $V_n = \mathrm{const}$) and differ in the initial phase and action. For all these particular cases, condition (9) of existence of the period-1 quasifixed points can be rewritten as
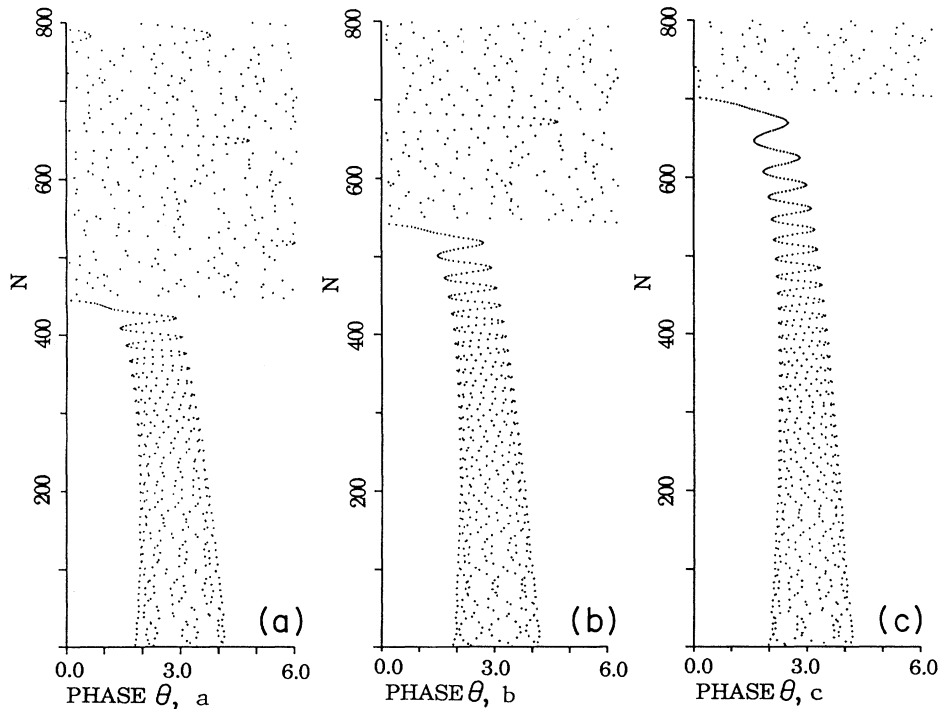
FIG. 1. Phase θ is shown as a function of n for the mapping (6), (7) with a constant δ_n, $\delta_n = -0.005$, $K_0 = 1$, i.e., $K_n = 0.995^n$. The initial conditions are (a) $J_0 = 6\pi + 0.2$, $\theta_0 = 4.1916$; (b) $J_0 = 4\pi + 0.2$, $\theta_0 = 4.1916$; (c) $J_0 = 2\pi + 0.2$, $\theta_0 = 4.1916$. From Eq. (16) (a) $N_\beta = 471$, (b) $N_\beta = 552$, and (c) $N_\beta = 690$.
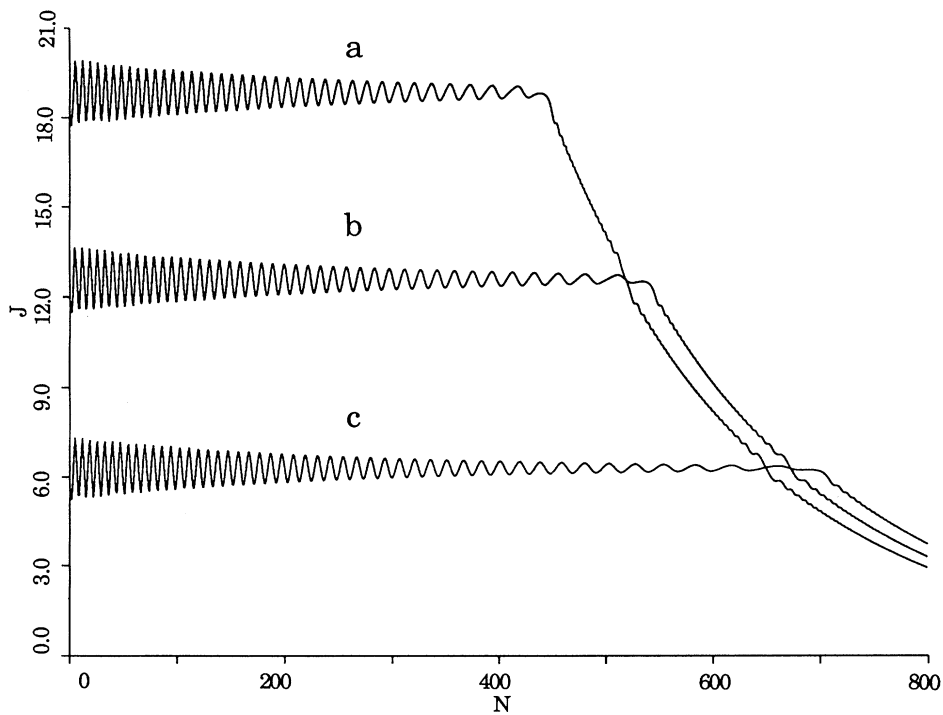
FIG. 2. J_n remains stable around $2\pi l$ ($l = 1, 2,$ and 3) until $n \approx N_\beta$. Then it is attracted to the eternal attractor at $J = 0$, $\theta = \pi$.
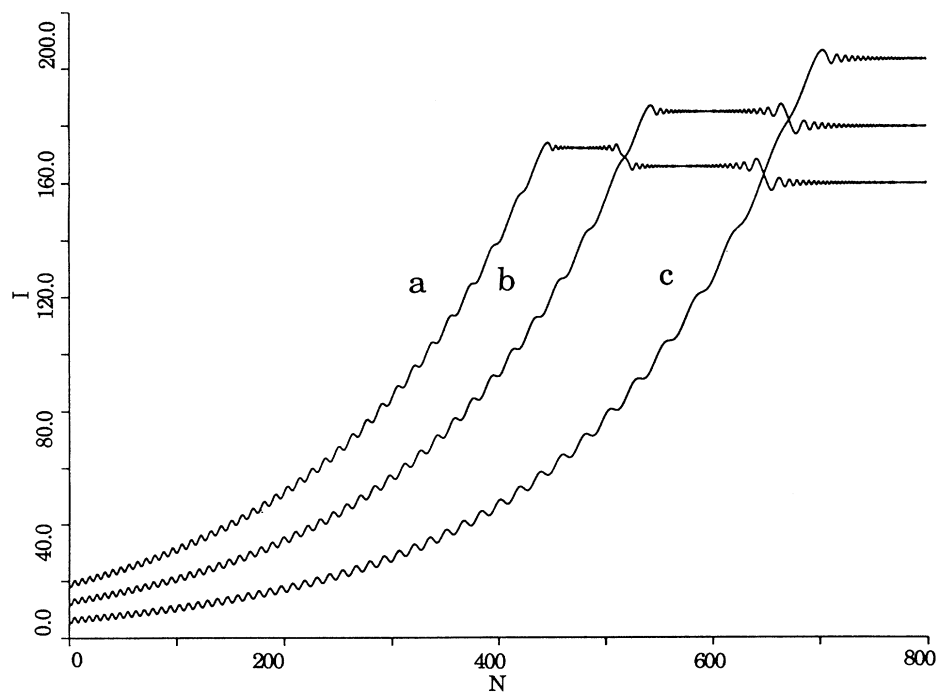
FIG. 3. Physical action I_n vs discrete time. The DAR acceleration is clearly seen. The breakdown points are the same as in Fig. 1. The growth of I agrees with Eq. (13).

$$n < n_\beta(l) = \ln(0.0052\pi l)/\ln(0,995). \qquad (16)$$

This condition breaks at $n_\beta = 690$, 552, and 471 in cases (a), (b), and (c), respectively. Figure 1 shows the evolution of phase θ_n with time. For all three trajectories the phase initially oscillates around θ_*. Also, the drift of θ_* is observed to proceed in agreement with Eq. (10), and the breakdown points are clearly seen to agree with Eq. (16) in all three cases. Figure 2 shows variable J_n, which oscillates with a decreasing amplitude around $2\pi l$, $l = 1$, 2, and 3. Figure 3 shows the evolution of the physical action I_n for the same trajectories. We observe that the autoresonance acceleration stops at n_β.

An *unlimited* acceleration can be achieved if variations of δ_n and K_{n+1} with n are chosen not to violate condition (9). An example of such a regime is shown in Figs. 4–6. We chose a simple relation between δ_n and K_{n+1}, $\delta_n = -K_{n+1}/5\pi$, and the logistic map (see, e.g., [7]) for K_{n+1}:

$$K_{n+1} = K_n \left[1 - \frac{K_n}{5\pi} \right]. \qquad (17)$$

In this case

$$\lim_{N \to \infty} \left[\frac{K_N}{K_0} \right] = 0 , \qquad (18)$$

$$\lim_{N \to \infty} \left[\frac{I_N}{I_0} \right] = \infty , \qquad (19)$$

and we achieve an unlimited acceleration, provided condition (9) is fulfilled. Indeed, it is easily seen that condition (9) never breaks down for the chosen value of δ_n and $l = 1$. The period-1 fixed point of the auxiliary mapping has $\theta_* = 2.73$ ($\sin\theta_* = 0.4$), and is independent of n; therefore it is also a "true" period-1 fixed point of mapping (6), (7). For $l > 2$, condition (9) is violated from the very beginning; therefore the acceleration on such l is impossible.

All these predictions agree well with our numerical calculations. Also, the calculations reveal a more complicated behavior of trajectories, initially close to separatrices. The latter includes both capture of initially free trajectories (i.e., those not lying within the island), and release of initially trapped ones. Figures 4–6 show θ, J, and I, respectively, as functions of n. We chose $K_0 = 1$ and considered three examples, denoted by (a), (b), and (c) and differing by the initial conditions. Trajectory (a) starts too far from any of the main islands. It passes by the resonances at $J = 4\pi$ and 2π and then continues towards the resonance $J = 0$ (see Fig. 5). Trajectory (b) starts near the separatrix of the $J = 4\pi$ resonance, and "falls" into the "stochastic sea," where it stays for some time until it is captured by the main island around $J = 2\pi$, where it stays forever. In this case the main island at $J = 2\pi$ acts like a trap. Trajectory (c) begins inside the $J = 2\pi$ island where it stays forever, oscillating around θ_* with a decreasing amplitude. Case (a) corresponds to an "untrapped" trajectory which is chaotic at the beginning but later becomes regular, since K_n slowly
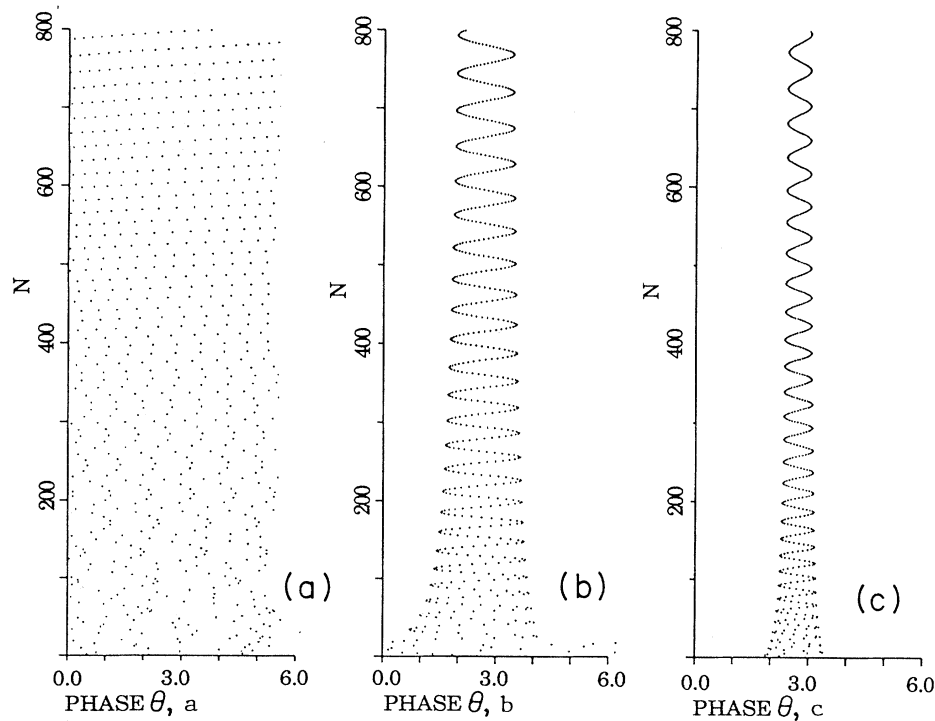
FIG. 4. Phase θ as a function of n as described by mapping (6), (7) with $\delta_n = -K_n/5\pi$, $K_0 = 1$ and the following initial conditions: (a) $J_0 = 6\pi + 0.2$, $\theta_0 = 3.48$; (b) $J_0 = 4\pi + 0.2$, $\theta_0 = 2.9643$; (c) $J_0 = 2\pi + 0.2$, $\theta_0 = 3.48$.
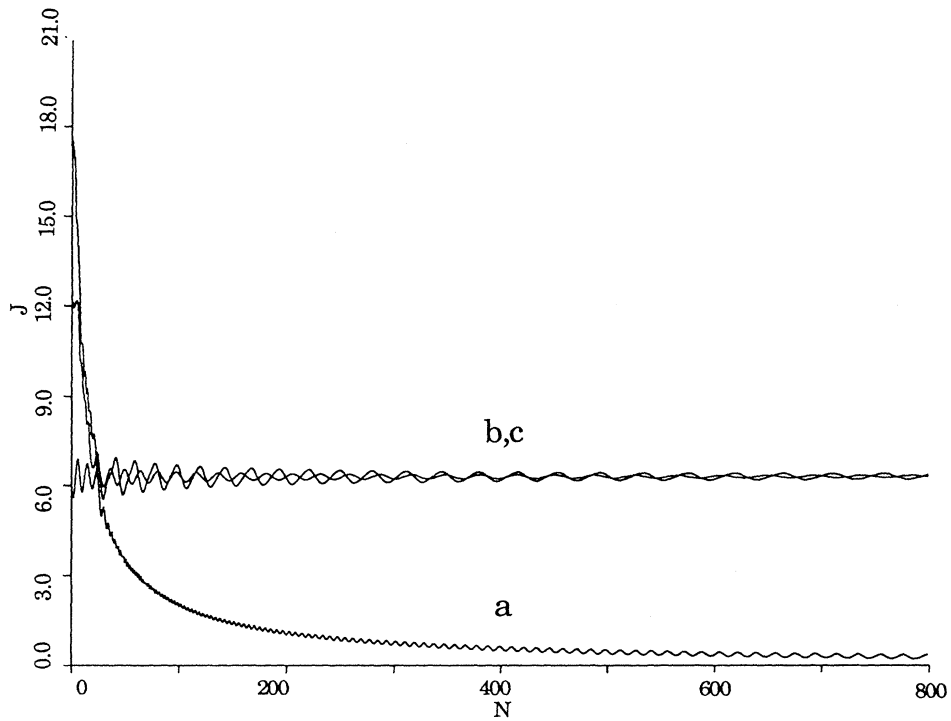
FIG. 5. Variable J as a function of n. The cases are the same as in Fig. 4. The smaller oscillations correspond to case (c).
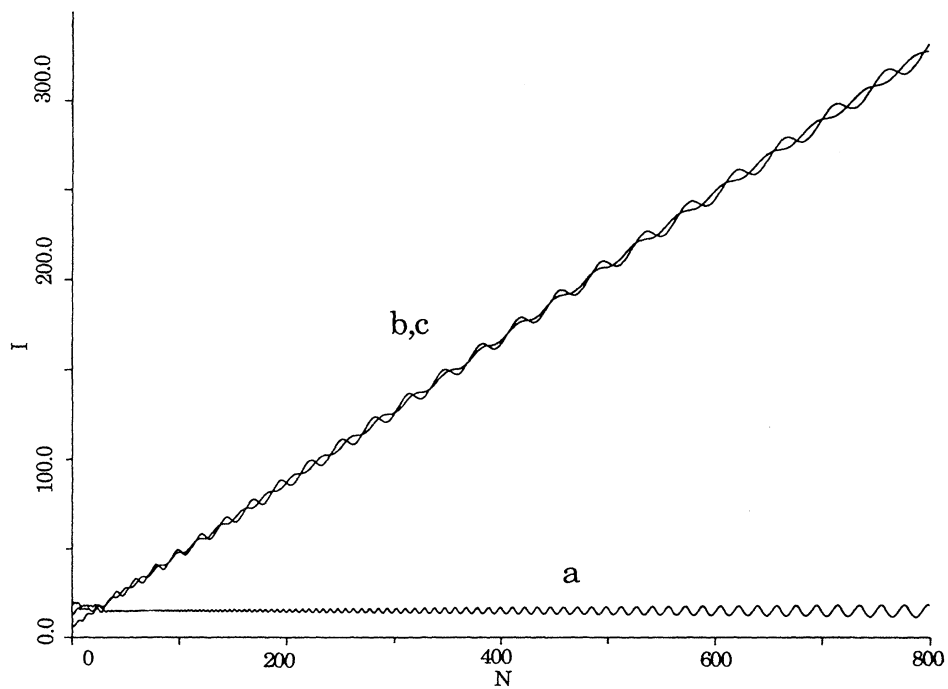
FIG. 6. Physical action I as a function of n. The cases are the same as in Figs. 4 and 5.

decreases from a value of $K_0 = 1$ to about $K_N = 0.02$. Cases (b) and (c) show sinusoidallike behavior with decreasing amplitude and frequency. As is seen from Fig. 6, in case (a) I oscillates around approximately a constant value (no DAR acceleration occurs). Trajectory (b) is caught into the DAR and gets accelerated, while (c) starts from autoresonance. In the cases (b) and (c), I_n grows, on the average, according to Eq. (13).

Of course, by a proper choice of δ_n / K_{n+1} we could satisfy condition (9) for any finite l. Note also that a dependence in which the δ_n / K_n ratio is kept constant is the only one which provides "true" (i.e., n-independent) period-1 fixed points of mapping (6), (7).

Higher-order islands corresponding to the quasifixed points of a higher order can also trap some trajectories, which leads to acceleration, transient or continuous. However, the condition of existence of these islands is more rigid than that for the main islands. We show in Figs. 7–9 three examples of trajectories for which we took $\delta_n = -K_n / 20\pi$ and $K_0 = 1$. Cases (a) and (b) show trajectories which are temporarily trapped by period-2 islands (Figs. 7 and 8) and thus involved in the (transient) DAR acceleration on the second harmonic of frequency ω (Fig. 9); see Eq. (15). In case (a), the period-2 island at $J = 3\pi$ ceases to exist at $n \approx 90$, then the trajectory bypasses the $J = 2\pi$ island, afterward the two $J = \pi$ islands, and then approaches $J = 0$. In case (b), the period-2 island at $J = \pi$ breaks down at $n \approx 550$. In contrast to cases (a) and (b), case (c) corresponds to the main island

and shows eternal stability (Figs. 7 and 8), leading to an unlimited acceleration (Fig. 9). The details of the phase behavior observed in case (a) are explained by the bypass of resonances $mJ = 2\pi l$, where m and l are integers. The eternal existence of the main island, one of which trajectories is shown in case (c), agrees with Eq. (9) and corresponds to $\theta_* = \pi - \sin^{-1}(0.1)$. For this trajectory we have, on the average, that $I_n / I_0 \approx K_0 / K_n \approx 7.2$ (see Fig. 9), in a good agreement with Eq. (13).

In order to provide a deeper insight into the DAR effect and draw a parallel with other models, let us follow Ref. [8] and employ a time-dependent version of the single resonance approximation. Before this, however, it is convenient to transform Hamiltonian (3) from the physical time t to a "new time" τ, such that $\tau = \tau(t)$ is a monotonic function and $\tau(t_k) = k$, so that in the new time the kick period becomes constant and equal to 1. We pay for this convenience by variation with time of the frequency of the unperturbed Hamiltonian H_0, which now becomes $\zeta(\tau)\omega(I)$, where $\zeta(\tau) = dt/d\tau$. Actually, $\tau(t)$ can be arbitrary *between* successive kicks, as long as $\tau(t_k) = k$. We can use this arbitrariness to choose $\zeta(k) = T_k$, which gives the following simple relation between ζ and ξ:
$$\xi_k = \zeta(k)\omega'.$$

Expanding the perturbation term of the Hamiltonian in the Fourier series over the harmonics of frequency 2π (the Fourier coefficients slowly varying with time) and keeping only the resonant term, corresponding to the (evolving in time) lth main island, we shall obtain the fol-
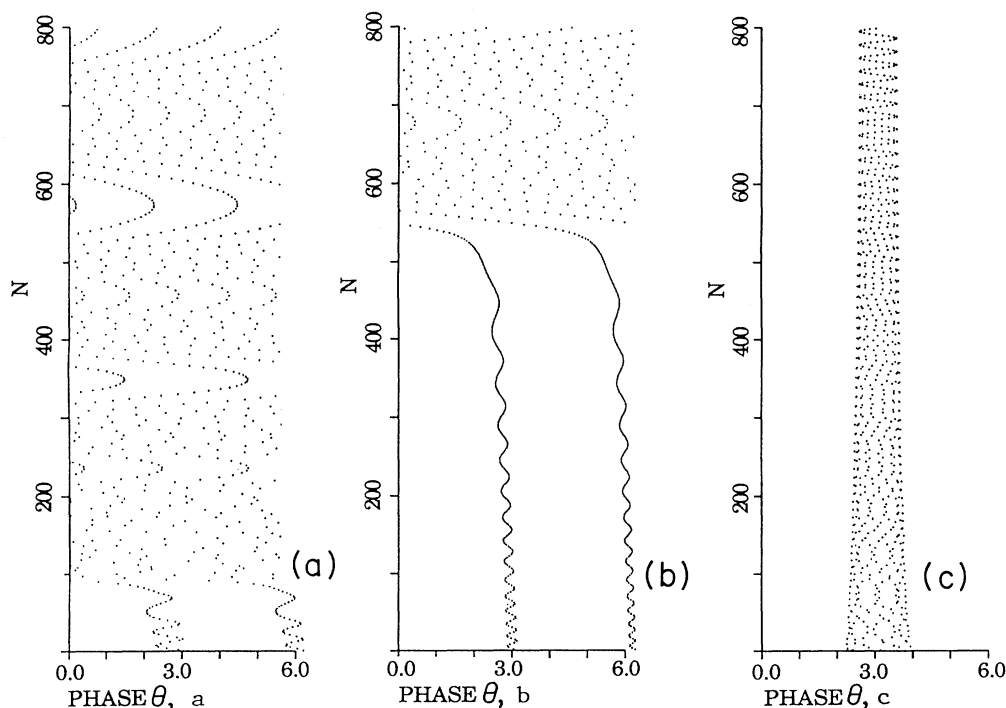
FIG. 7. Phase θ as a function of n as described by mapping (6), (7) with $\delta_n = -K_n / 20\pi$, $K_0 = 1$, and the following initial conditions: (a) $J_0 = 3\pi$, $\theta_0 = 3.0816$; (b) $J_0 = \pi$, $\theta_0 = \pi$; (c) $J_0 = 2\pi$, $\theta_0 = 3.6416$.
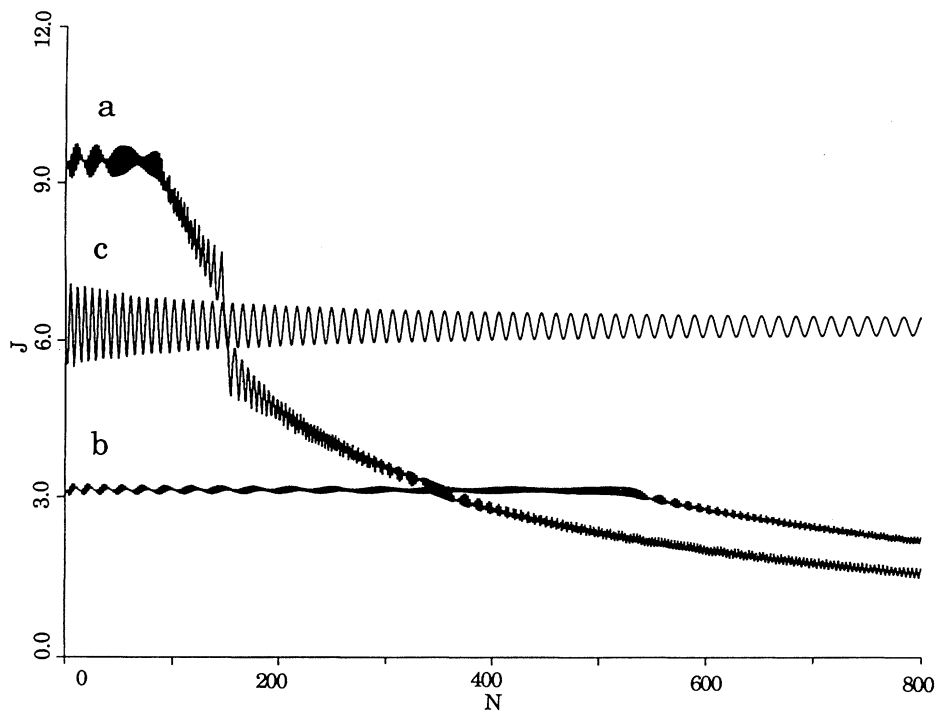
FIG. 8. Variable J as a function of n. The cases are the same as in Fig. 7.
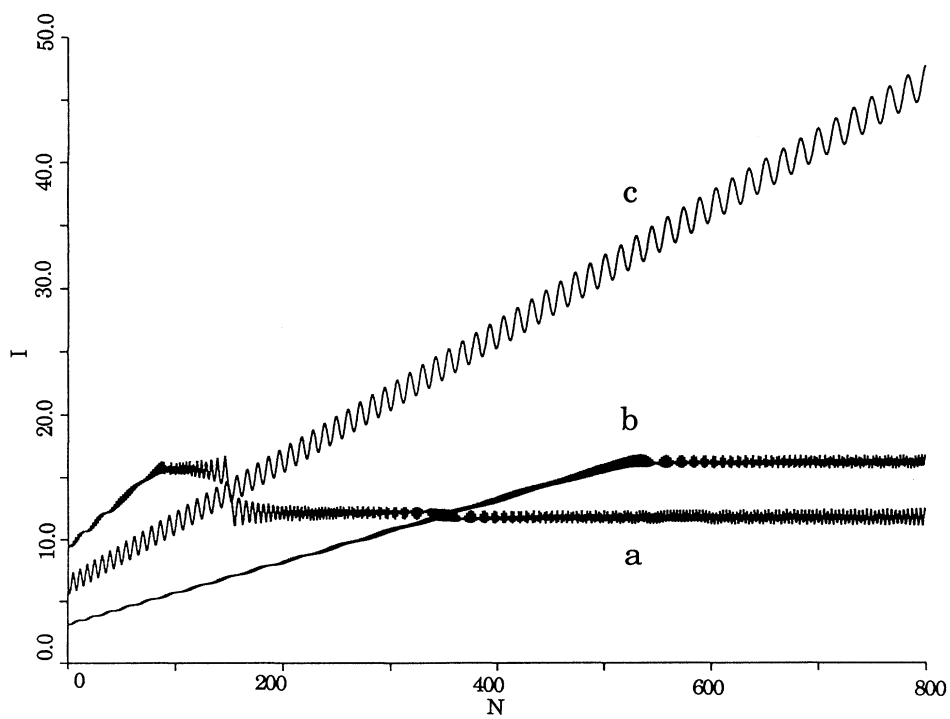
FIG. 9. Physical action I as a function of n. The cases are the same as in Figs. 7 and 8.

lowing canonical equations of motion in the vicinity of the lth resonance:

$$\dot{I} = -V(\tau)\sin(\theta - 2\pi m\tau) \ , \tag{20}$$

$$\dot{\theta} = \xi(\tau)\omega_0(I(\tau)) \ , \tag{21}$$

where $V(\tau) = V_k(\tau = k)$. Let us define a new phase

$$\psi(\tau) = \theta - 2\pi m\tau + \pi \tag{22}$$

and consider a rigid rotator for which $\omega_0(I) = I$ and hence $\xi_k = \zeta(k)$. Then, defining

$$J(\tau) = \xi(\tau)I(\tau) \ , \tag{23}$$

we arrive at the following equations of motion:

$$\dot{J} = \frac{\dot{\xi}}{\xi}J - \xi V(\tau)\sin\psi \ , \tag{24}$$

$$\dot{\psi} = J - 2\pi m \ , \tag{25}$$

which yield

$$\ddot{\psi} + V\xi(\sin\psi - \sin\psi_s) = \frac{\dot{\xi}}{\xi}\dot{\psi} \tag{26}$$

with

$$\psi_s = \arcsin\frac{2\pi n\dot{\xi}}{V\xi^2} \ . \tag{27}$$

We have assumed that $|2\pi m\dot{\xi}/V\xi^2| < 1$ since only in this

case there exist stable fixed points of Eqs. (24) and (25). This condition corresponds to condition (9) for the auxiliary mapping.

Equation (26) was encountered in various physical problems, such as, for example, particle dynamics in the synchrotron [4,9] and interaction between the electromagnetic wave and electrons in the free-electron laser [10]. If the corresponding time dependences of the parameters in Eq. (27) are slow on the time scale of the oscillation frequency, the solution for the trapped, or phase-locked, particles has the character of oscillations with slowly varying amplitude and frequency.

Equations (24)–(26) describe a particle motion in a slowly time-dependent potential

$$\Psi = V\xi(\cos\psi_s + \psi_s\sin\psi_s - \cos\psi - \psi\sin\psi_s) \tag{28}$$

with the friction force

$$F_{\text{diss}} = \frac{\dot{\xi}}{\xi}\dot{\psi} \ . \tag{29}$$

Now, defining kinetic energy

$$T = \tfrac{1}{2}(J - 2\pi m)^2 \ , \tag{30}$$

we see that the "total energy"

$$\Phi = T + \Psi \tag{31}$$

is a slow function of time. This fact enables us to esti-
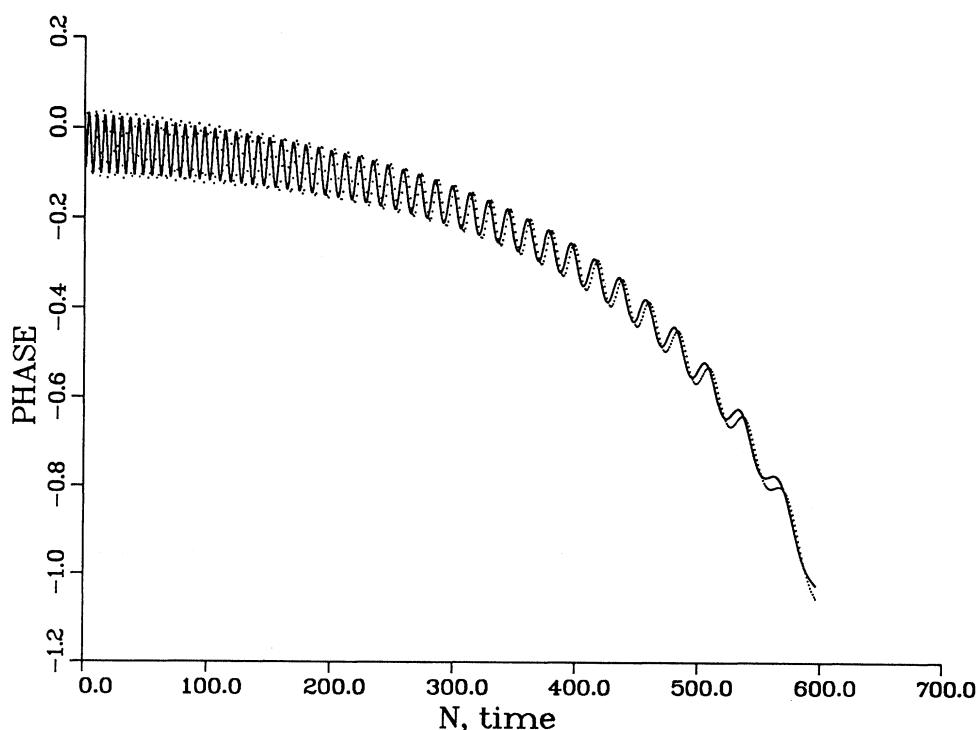
FIG. 10. Comparison between mapping (6), (7) and the solution of Eq. (26), with $K_0 = 1.0$, $\delta = -0.0054 = $const, $\theta_0 = \pi - 0.1$, and $I_0 = 2\pi$.

mate the resonance width, if we neglect the slow time dependences. For the trapped trajectories, the phase is confined between a local maximum of potential Ψ, say ψ_1, and another phase ψ_2 for which

$$\Psi(\psi_1) = \Psi(\psi_2) \ . \tag{32}$$

Using Eq. (28), we see that

$$\psi_1 = \pi \operatorname{sgn}\psi_s - \psi_s \ . \tag{33}$$

Substituting it into Eq. (28) we obtain

$$\Phi(\psi_1) = V\xi[2\cos\psi_s + (2\psi_s - \pi\operatorname{sgn}\psi_s)\sin\psi_s] \ , \tag{34}$$

while ψ_2 is found from the following transcendental equation:

$$\cos\psi_s + \cos\psi_2 + (\psi_2 + \psi_s - \pi\operatorname{sgn}\psi_s)\sin\psi_s = 0 \ . \tag{35}$$

From Eqs. (30), (31), and (34) we obtain the resonance width, or the island size, by which we call the maximum amplitude of oscillations of J:

$$\Delta J = \{2V\xi[2\cos\psi_s + (2\psi_s - \pi\operatorname{sgn}\psi_s)\sin\psi_s]\}^{1/2} \ . \tag{36}$$

For a fixed period of the kicks we have $\psi_s = 0$, and Eq. (36) gives the well-known result [1–3] $\Delta J = (4K)^{1/2}$. It can be seen from Eqs. (36) and (27) that the resonance width decreases with an increase of m, and becomes zero as ψ_s approaches $+\pi/2$ or $-\pi/2$.

We have solved Eq. (26) numerically for $K_0 = 1.0$ and $\delta = 0.0054 = \text{const}$ for some typical initial conditions and compared the results with those of mapping (6), (7). Figure 10 shows a typical example of this comparison for an initial condition corresponding to a main island. The close similarity between the evolution of phase as described by mapping (6), (7), and the single resonance equation (26) is clearly seen.

III. DYNAMIC AUTORESONANCE AND "DRAGGING" TO GLOBAL CHAOS

In this section we briefly consider the DAR in the case of a slowly *increasing* kick period. There are two physical situations which make such a case interesting. Energization of a nonlinear oscillator with a *negative* nonlinearity presents the first one, and deceleration of and extraction of energy from an oscillator with a positive nonlinearity (in the simplest case, rigid rotator) presents the second.

In the first case, the unperturbed Hamiltonian $H_0(I)$ [see Eq. (3)] is such that $d\omega/dI < 0$. To be more specific, let us consider the following example:

$$H_0(I) = \omega_0 I - \left[\frac{\gamma}{2}\right]I^2 \ , \quad \gamma > 0 \tag{37}$$

therefore $\omega(I) = \omega_0 - \gamma I$. Assume that we start from some $I_0 < I_{\max} = \omega_0/\gamma$. Keeping in mind that $\omega' = (-\gamma) < 0$, and transforming to the new variables according to

$$J_n = \omega_0 T_n - \gamma T_n I_n \ , \tag{38}$$

$$\phi_n = \theta_n + \pi \ , \tag{39}$$

we arrive once again at mapping (6), (7) with ϕ instead of θ [all the notation remains the same except that now $\xi_n = \gamma T_n$, and J_n is given by Eq. (38)]. This means that the DAR acceleration is possible in this case as well. However, there are some differences. The first of them is an artifact of the specific model (37): the constancy of $\langle J_n \rangle = J_* = 2\pi l$ now means that

$$I_n \approx I_{\max} - \frac{J_n}{\xi_n} \ , \tag{40}$$

i.e., I_n is limited: $I_n < I_{\max} = \omega_0/\gamma$ if ξ_n is growing with n.

Second, the case of an increasing T_n corresponds to $\delta_n > 0$, therefore mapping (6), (7) is characterized by a negative dissipation. The absolute values of the two eigenvalues of the tangent mapping, corresponding to the period-1 fixed points of the auxiliary mapping, are now larger than 1 [see Eq. (11)]. This means that trajectories initially close to the period-1 fixed point will move outward. In our numerical simulations we see this tendency holding for all the trajectories inside the islands that we checked.

Third, since $K_{n+1} = V_n\xi_{n+1}$, the growth of ξ_n leads to the growth of K_{n+1} (unless V_n decreases too fast). As K_{n+1} reaches $K_{\text{crit}}(l)$ from Eq. (12), the main island loses its stability. In the case of the standard mapping, the loss of stability of a period-1 fixed point at $K = 4$ is accompanied by the birth of two stable period-2 fixed points by bifurcation [1–3]. Therefore, in the case of mapping (6), (7) with (adiabatically) slowly varying parameters, we can expect a process of doubling bifurcation to occur at some discrete time moment n, when stability criterion (12) breaks [if condition (9) for the existence of the period-1 fixed point still holds]. Similarly, we can expect a series of multiplying bifurcations and the transition to global chaos to develop *in time*, as parameter K_{n+1} is slowly increasing. These effects are indeed seen in our numerical simulations. Figures 11–13 show how the motion in the
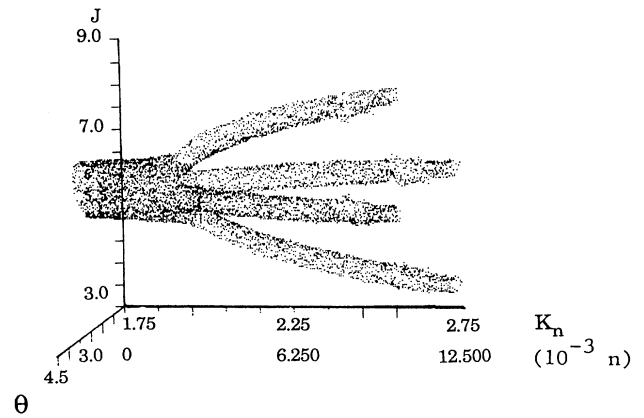
FIG. 11. Extended phase space (θ, I, n) as described by mapping (6), (7). $K_0 = 1.75$, $K_{n+1} - K_n = 8 \times 10^{-5} = \text{const}$, $\theta_0 = 2.72$, and $I_0 = 6.3$.
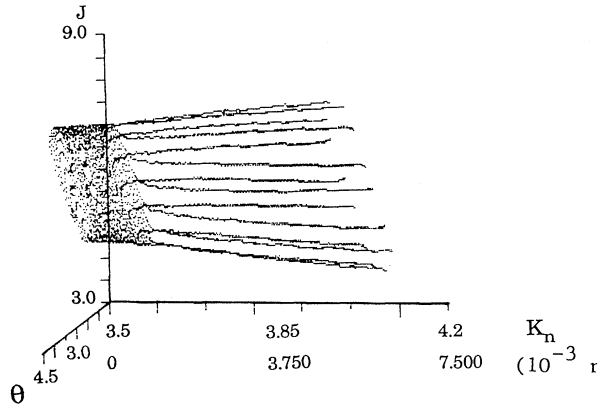
FIG. 12. Same as Fig. 11, but now $K_0 = 3.5$, $K_{n+1} - K_n = 8 \times 10^{-5} = $ const, $\theta_0 = 2.75$, and $I_0 = 6.25$.

plane (I, θ) changes with the discrete time n. In each of Figs. 11–13, we show a single trajectory, generated by mapping (6), (7).

In Fig. 11 we use mapping (6), (7) with $K_n = 1.75 + 8 \times 10^{-5} n$, $\delta_n = 8 \times 10^{-5}/(1.75 + 8 \times 10^{-5} n)$ for the total number of steps $N = 12\,500$. At $K_n \approx 2.05$ we see a bifurcation of the trajectory, related to the appearance of secondary islands near the separatrix of the main island.

In Fig. 12 we chose $K_n - K_{n-1} = 3.5 + 8 \times 10^{-5} n$, $\delta_n = 8 \times 10^{-5}/(3.5 + 8 \times 10^{-5} n)$ and $N = 7500$. At $K_n \approx 3.7$ we see bifurcation of the single trajectory into period-14 secondary islands which also lie near the separatrix of the main island with $K = 3.7$. At $n \approx 8000$ this trajectory becomes chaotic (not shown in Fig. 12).

Figure 13 corresponds to $K_n = 3.8 + 8 \times 10^{-5} n$, $\delta_n = 8 \times 10^{-5}/(3.8 + 8 \times 10^{-5} n)$, and $N = 12\,500$. Equation (12) predicts bifurcation of the main island into two period-2 islands at $K_n \approx 4.000\,02$. This bifurcation is clearly observed in Fig. 13 as occurring at the time moment $n \approx 2500$, in a good agreement with Eq. (12).
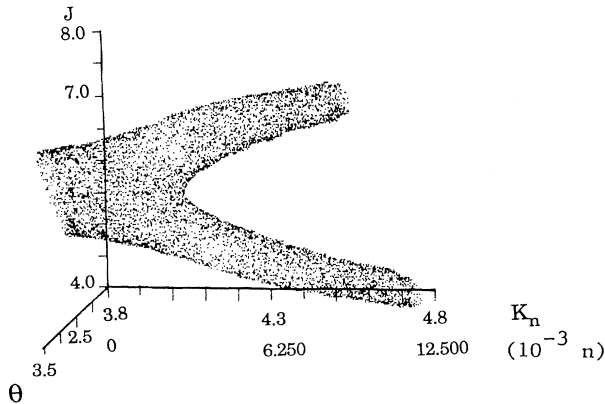
FIG. 13. Same as Fig. 11, but with $K_0 = 3.8$, $K_{n+1} - K_n = 8 \times 10^{-5} = $ const, $\theta_0 = 3.24$, and $I_0 = 6.25$.

IV. NONSTATIONARY DIFFUSION IN THE ACTION SPACE

In this section we consider the case of a well-developed time-dependent global chaos in mapping (6), (7) and study the nonstationary diffusion in the action space.

In the limit of $K \gg 1$, the behavior of the action variable of the standard mapping is quite accurately described by the following "quasilinear" diffusion equation [11, 12]:

$$\frac{\partial}{\partial n} \rho(I, n) = \mathcal{D}(K) \frac{\partial^2}{\partial I^2} \rho , \qquad (41)$$

which gives the following solution for the mean square of ΔI:

$$\langle (\Delta I_n)^2 \rangle = n \mathcal{D}(K) . \qquad (42)$$

The diffusion coefficient $\mathcal{D}(K)$ is given by equation

$$\mathcal{D}(K) = K^2 [0.5 - J_2(K) - J_1^2(K) + J_2^2(K) + J_3^2(K)] , \qquad (43)$$

where J_p is the Bessel function of the pth order (see Ref. [2] and references therein). The diffusion coefficient (43) is an oscillating function of K, the oscillation period being close to 2π at $K \gg 1$. Dividing Eq. (1) by K and denoting $I_{new} = I/K$, we see that the diffusion of I_{new} is characterized by the diffusion coefficient $\mathcal{D}(K)/K^2$, which is just the term inside the square brackets of Eq. (43).

Similarly, we can treat the modified standard mapping (4), (5). Taking $\omega(I) = \omega_0 + \omega' I$ with positive ω_0 and ω', changing variables from I to $I' = I + (\omega_0/\omega')$, and setting for simplicity $V_n = $ const $= 1$, we arrive at the following mapping:

$$I_{n+1} = I_n + \sin\theta_n , \qquad (44)$$

$$\theta_{n+1} = \theta_n + \xi_{n+1} I_{n+1} \qquad (45)$$

which is similar to the standard mapping (1), (2) with divided-by-K Eq. (1), ξ_{n+1} playing the role of K. The difference consists in the n dependence of ξ_{n+1}. If this dependence is very slow and $\xi_{n+1} \gg 1$, we can still describe the system in terms of diffusion in the action space but the diffusion coefficient becomes n dependent (i.e., discrete time dependent). Therefore the evolution of the distribution function of I as a function of the discrete time n, $\rho(I, n)$, must satisfy the following equation:

$$\frac{\partial}{\partial n} \rho = \mathcal{D}(n) \frac{\partial^2}{\partial I^2} \rho , \qquad (46)$$

where the diffusion coefficient $\mathcal{D}(n)$ is given by Eq. (43), where K is replaced by ξ_{n+1}. The linear diffusion equation (45) with a time-dependent diffusion coefficient can be easily solved analytically. In particular, if we start with the simplest initial condition $\rho(I, 0) = \delta(I)$, where δ is the Dirac delta function, the solution of Eq. (45) predicts that

$$\langle (\Delta I_n)^2 \rangle = \int_0^n \mathcal{D}(t) dt . \qquad (47)$$
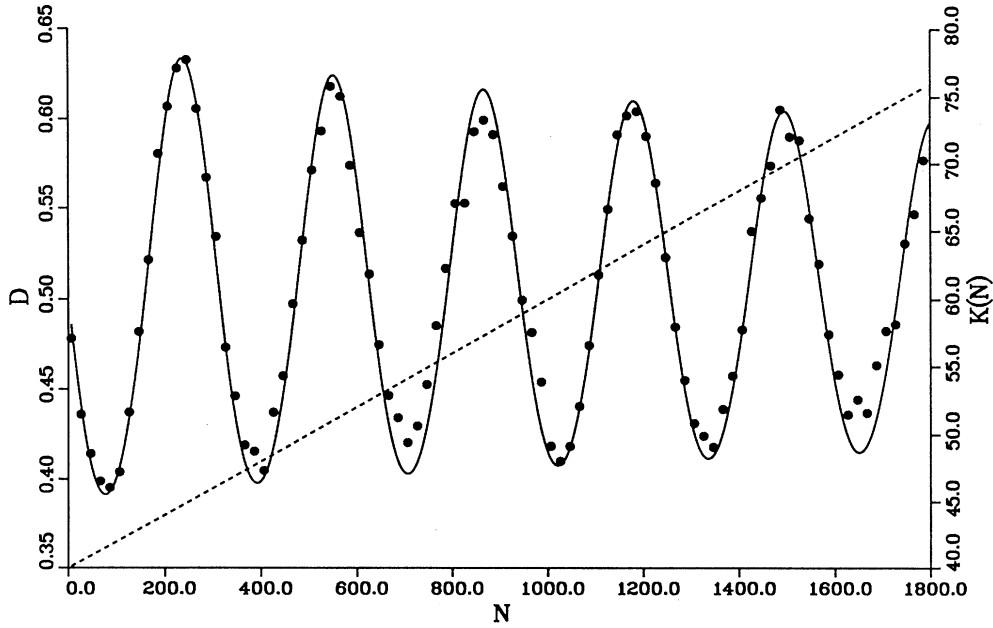
FIG. 14. Diffusion coefficient $\mathcal{D}$ (solid line and dots) and stochasticity parameter $K_N = 40 + N/50$ (dashed line) as functions of N. Solid line, $\mathcal{D}$ as calculated from Eq. (42); dots, $\mathcal{D}$ computed from mapping (37), (38) via averaging over 1.5×10^6 initial conditions.

In order to check this prediction, we performed numerical simulations with mapping (43), (44),where we used an ensemble of 1.5×10^6 trajectories. The time-dependent diffusion coefficient was computed as the (numerical) first derivative of the mean square of ΔI_n:

$$\mathcal{D}(n) = \frac{\partial}{\partial n} \langle (\Delta I_n)^2 \rangle . \tag{48}$$

Figure 14 shows $\mathcal{D}$ calculated from Eq. (43) versus that calculated from Eq. (48). The agreement is quite good. It is worth mentioning that, in contrast to the standard mapping, where it is necessary to introduce some amount of noise in order to eliminate the contributions of the accelerator modes [11], the computation procedure here is straightforward, because the acceleration modes are absent.

V. EXAMPLE

A simple example for which the modified standard mapping can be applied is provided by an absolutely elastic ball bouncing on a vertically vibrating floor. The case of a constant vibration frequency of the floor was considered by Pustylnikov [13] and Holmes [14] as a model for Fermi acceleration. Let us consider the case of a slowly varying frequency of the floor vibration and demonstrate the DAR effect in this simple system. Assume that the vibration amplitude is small, and let $\Omega(t)$ and $U(t)$ be the time-dependent vibration frequency and the floor velocity, respectively:

$$U(t) = U_0 \sin\varphi(t) , \tag{49}$$

where

$$\varphi(t) = \int_0^t \Omega(t')dt' . \tag{50}$$

If we denote the ball velocity at the instance when it hits the floor for the kth time by u_k, we shall obtain the following relations:

$$u_{k+1} = u_k + 2U_0 \sin\varphi_k , \tag{51}$$

$$\varphi_{k+1} = \varphi_k + \frac{2\Omega_{k+1}}{g} u_{k+1} , \tag{52}$$

where g is the gravitational acceleration and Ω_{k+1} is the average floor vibration frequency between the kth and the $(k+1)$th hit on the floor:

$$\Omega_{k+1} = \frac{g}{2u_{k+1}} \int_{T_n}^{T_{n+1}} \Omega(t')dt' . \tag{53}$$

The problem is reduced to mapping (4), (5) after introducing

$$J_n = \frac{2}{g} \Omega_n u_n , \tag{54}$$

$$K_n = \frac{4U_0}{g} \Omega_n . \tag{55}$$

For example, if the floor vibration frequency is initially close to the ball's bounce-frequency [Eq. (14) with $l = 1$] and U_0 is not too large [so that inequality (12) is satisfied], criterion (9) becomes

$$\frac{\pi^2 g |\dot{\Omega}|}{\Omega^3 U_0} < 1 , \tag{56}$$

so that by slowly decreasing the floor vibration frequen-

cy, we can "lock" the ball's bounce frequency and accelerate the ball.

VI. SUMMARY

We investigated numerically and analytically the dynamics of a rigid rotator under the action of kicks, when both the strength of the kicks and the interval between them (the kick period) vary with time. We developed a "modified standard map" for this model and, within its framework, provided a simpler and more detailed description of three rather general effects. The first of them, which has been well known for some time in different physical systems, is dynamic autoresonance, or dynamic phase locking. We found a set of conditions (existence and stability of the quasifixed points) for which the effect occurs. In particular, we found the condition under which the DAR acceleration proceeds unlimitedly.

Second, we investigated the time-dependent transition to global chaos that arises due to the increase of the stochasticity parameter K with time. We found that this transition occurs through bifurcation of the main island

at $K = K_{crit}$ (the bifurcation parameter being simply time) and the development of a complicated separatrix structure.

Third, we employed a time-dependent diffusion equation, generalizing the quasilinear equation found earlier for the standard mapping, to describe the time-evolving global chaos. This equation has been found to agree very well with our numerical simulations.

Finally, we presented a simple physical example of an elastic ball bouncing on an oscillating floor with a variable oscillation frequency, and showed that the problem can be described by the modified standard mapping (4), (5).

In conclusion, the kicked rotator with slowly varying kicks provides a convenient model of studying generic phenomena of the DAR and DAR-induced global chaos in driven nonlinear systems with slowly varying parameters.

[1] B. V. Chirikov, Phys. Rep. **52**, 263 (1978).
[2] A. J. Lichtenberg and M. A. Lieberman, *Regular and Stochastic Motion* (Springer-Verlag, New York, 1983).
[3] R. Z. Sagdeev, D. A. Uzikov, and G. M. Zaslavsky, *Nonlinear Physics. From the Pendulum to Turbulence and Chaos* (Harwood Academic, Chur, 1988).
[4] D. Bohm and L. L. Foldy, Phys. Rev. **70**, 649 (1947).
[5] I. Dana and W. P. Reinhardt, Physica D **28**, 115 (1987).
[6] G.M. Zaslavsky, Phys. Lett. **69A**, 145 (1978).
[7] P. Collet and J. P. Eckmann, *Progress in Physics* (Birkhäuser Verlag, Basel, 1980), Vol. 1.
[8] B. Meerson and L. Friedland, Phys. Rev. A **41**, 5233

(1990).
[9] J. Rosenblatt, *Particle Acceleration* (Mathuen, London, 1968).
[10] T. C. Marshall, *Free-Electron Lasers* (Macmillan, New York, 1985).
[11] A. B. Rechester and R. B. White, Phys. Rev. Lett. **44**, 1586 (1980).
[12] A. B. Rechester, M. N. Rosenbluth, and R. B. White, Phys. Rev. A **23**, 2664 (1981).
[13] L. D. Pustylnikov, Trans. Moscow Math. Soc. **2**, 1 (1978).
[14] P. J. Holmes, J. Sound Vib. **84**, 173 (1982).